

# The pseudoparticle approach in SU(2) Yang-Mills theory

Marc Wagner

[mcwagner@physik.hu-berlin.de](mailto:mcwagner@physik.hu-berlin.de)

<http://people.physik.hu-berlin.de/~mcwagner/>

May 22, 2006

# Outline

## **Part I: the pseudoparticle approach, a model for SU(2) Yang-Mills theory**

- Basic principle.
- Numerical results: static quark antiquark potential, topological susceptibility, critical temperature.

## **Part II: properties of confining gauge field configurations**

- Pseudoparticles of different size and profile.
- Instantons, antiinstantons and skyrmions.

## **Part III: fermions in the pseudoparticle approach (work in progress)**

- Problems with fermionic fields in the pseudoparticle approach.
- The Gross-Neveu model as testing ground.

## **Summary and outlook**

# Part I: the pseudoparticle approach, a model for $SU(2)$ Yang-Mills theory

# Basic principle (1)

- Pseudoparticle approach (PP approach; F. Lenz, M.W., 2005):
  - A numerical technique to approximate Euclidean path integrals (in this talk: mainly SU(2) Yang-Mills theory):

$$\langle \mathcal{O} \rangle = \frac{1}{Z} \int DA \mathcal{O}[A] e^{-S[A]}$$

$$S[A] = \frac{1}{4g^2} \int d^4x F_{\mu\nu}^a F_{\mu\nu}^a, \quad F_{\mu\nu}^a = \partial_\mu A_\nu^a - \partial_\nu A_\mu^a + \epsilon^{abc} A_\mu^b A_\nu^c.$$

- A tool to analyze the importance of certain classes of gauge field configurations with respect to confinement.
- Related work:
  - \* Ensembles of regular gauge instantons and merons (F. Lenz, J. W. Negele, M. Thies, 2003).
  - \* Ensembles of calorons with non-trivial holonomy (P. Gerhold, E.-M. Ilgenfritz, M. Müller-Preussker, 2006).

# Basic principle (2)

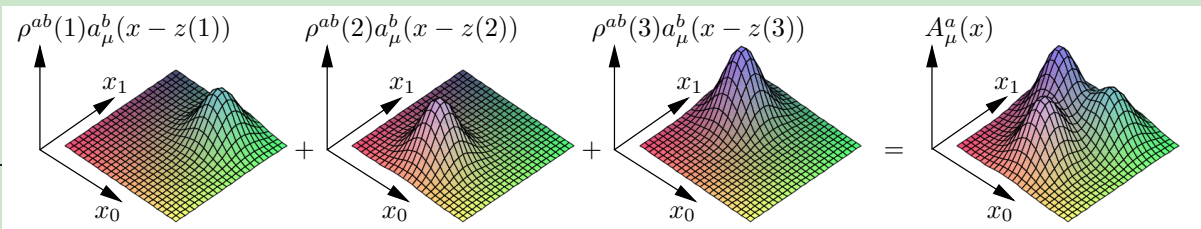
- PP: any gauge field configuration  $a_\mu^a$ , which is localized in space and in time.
- Consider only those gauge field configurations, which can be written as a sum of a fixed number ( $\approx 400$ ) of PPs:

$$A_\mu^a(x) = \sum_j \rho^{ab}(j) a_\mu^b(x - z(j))$$

( $j$ : PP index;  $\rho^{ab}(j)$ : degrees of freedom of the  $j$ -th PP, i.e. amplitude and color orientation;  $z(j)$ : position of the  $j$ -th PP).

- Define the functional integration as an integration over the PP degrees of freedom:

$$\int DA \dots \rightarrow \int \left( \prod_j d\rho^{ab}(j) \right) \dots$$



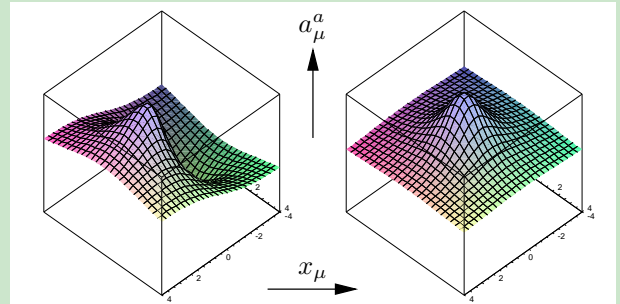
# Building blocks of PP ensembles

- Building blocks of PP ensembles: “instantons”, “antiinstantons”, akryons ( $\lambda$ : PP size).

$$a_{\mu,\text{instanton}}^a(x) = \eta_{\mu\nu}^a \frac{x_\nu}{x^2 + \lambda^2}$$

$$a_{\mu,\text{antiinstanton}}^a(x) = \bar{\eta}_{\mu\nu}^a \frac{x_\nu}{x^2 + \lambda^2}$$

$$a_{\mu,\text{akryon}}^a(x) = \delta^{a1} \frac{x_\mu}{x^2 + \lambda^2}.$$



- Instantons, antiinstantons and akryons form a basis of all gauge field configurations in the “continuum limit”.
- Degrees of freedom: amplitudes  $\mathcal{A}(i)$ , color orientations  $\mathcal{C}^{ab}(i)$ , positions  $z(i)$ .

$$A_\mu^a(x) = \mathcal{A}(i)\mathcal{C}^{ab}(i)a_{\mu,\text{instanton}}^a(x - z(i))$$

$$A_\mu^a(x) = \mathcal{A}(i)\mathcal{C}^{ab}(i)a_{\mu,\text{antiinstanton}}^a(x - z(i))$$

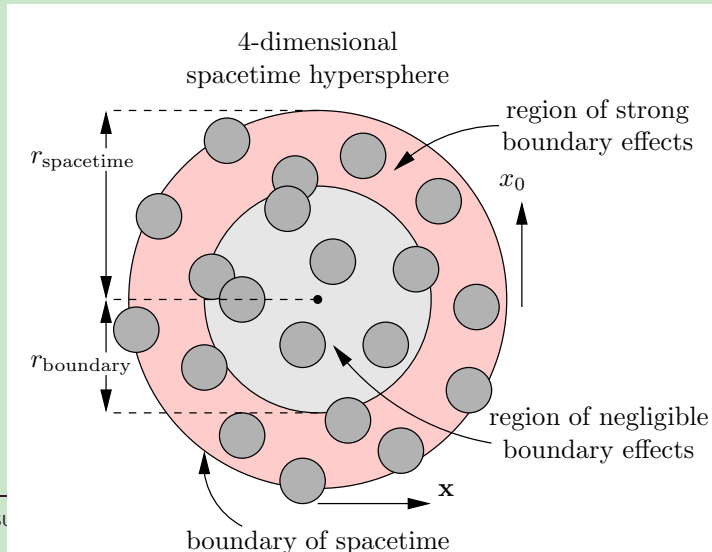
$$A_\mu^a(x) = \mathcal{A}(i)\mathcal{C}^{ab}(i)a_{\mu,\text{akryon}}^a(x - z(i)).$$

# PP ensembles (1)

- PP ensemble: a fixed number of PPs inside a spacetime hypersphere.
- Gauge field:

$$A_{\mu}^a(x) = \sum_i \mathcal{A}(i) \mathcal{C}^{ab}(i) a_{\mu, \text{instanton}}^b(x - z(i)) + \sum_j \mathcal{A}(j) \mathcal{C}^{ab}(j) a_{\mu, \text{antiinstanton}}^b(x - z(j)) + \sum_k \mathcal{A}(k) \mathcal{C}^{ab}(k) a_{\mu, \text{akyron}}^b(x - z(k)).$$

- Choose color orientations  $\mathcal{C}^{ab}(i)$  and positions  $z(i)$  randomly.
- $A_{\mu}^a$  is no classical solution (not even close to a classical solution)!
- Long range interactions between PPs.



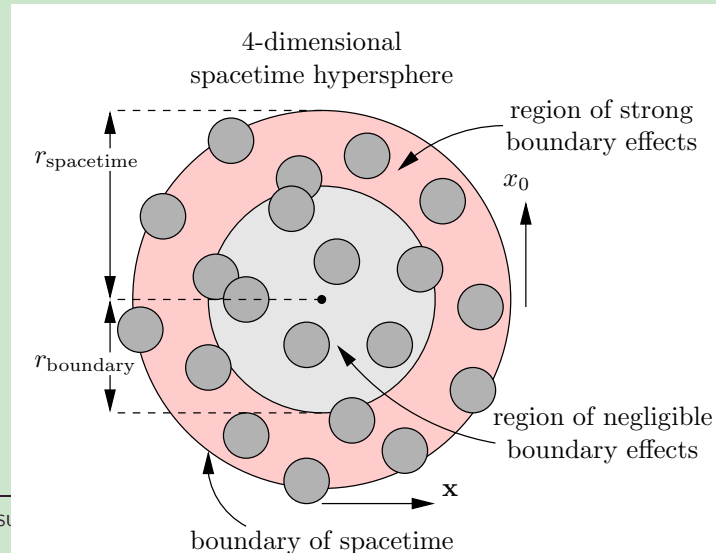
# PP ensembles (2)

- Approximation of the path integral:

$$\langle \mathcal{O} \rangle = \frac{1}{Z} \int \left( \prod_i d\mathcal{A}(i) \right) \mathcal{O}(\mathcal{A}(i)) e^{-S(\mathcal{A}(i))}$$

(integration over PP amplitudes).

- Solve this multidimensional integral via Monte-Carlo simulations.
- Exclude boundary effects: observables have to be “measured” sufficiently far away from the boundary.





# Quark antiquark potential (1)

- Common tool to determine the potential of a static quark antiquark pair: Wilson loops ( $z$ : closed spacetime curve),

$$W_z[A] = \frac{1}{2} \text{Tr} \left( P \left\{ \exp \left( i \oint dz_\mu A_\mu(z) \right) \right\} \right).$$

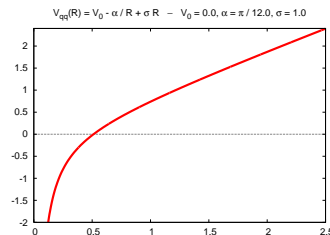
- Rectangular Wilson loop ( $R, T$ : spatial and temporal extension):  $W_{(R,T)}$ .
- Wilson loops  $\leftrightarrow$  quark antiquark potential ( $R$ : quark antiquark separation):

$$V_{q\bar{q}}(R) = - \lim_{T \rightarrow \infty} \frac{1}{T} \ln \langle W_{(R,T)} \rangle.$$

- Assumption: the potential for large quark antiquark separations can be parameterized according to

$$V_{q\bar{q}}(R) = V_0 - \frac{\alpha}{R} + \sigma R.$$

$V_{q\bar{q}}$  plotted against  $R$



# Quark antiquark potential (2)

**Method 1: Determine the string tension  $\sigma$  and the Coulomb coefficient  $\alpha$**

- “Guess” the functional dependence of ensemble averages of Wilson loops:

$$-\ln \langle W_{(R,T)} \rangle = V_0(R+T) - \alpha \left( \frac{R}{T} + \frac{T}{R} \right) + \beta + \sigma RT.$$

- Determine the string tension  $\sigma$  and the Coulomb coefficient  $\alpha$  by fitting the “Wilson loop ansatz” to Monte-Carlo data for  $-\ln \langle W_{(R,T)} \rangle$ .
- Several approaches:
  - Area perimeter fits.
  - Creutz ratios.
  - Generalized Creutz ratios.
  - ...

# Quark antiquark potential (3)

**Method 1: Determine the string tension  $\sigma$  and the Coulomb coefficient  $\alpha$**

- Parameterization of the quark antiquark potential:

$$V_{q\bar{q}}(R) = V_0 - \frac{\alpha}{R} + \sigma R.$$

- Results for PP ensembles containing  $\approx 400$  PPs:

- **String tension  $\sigma > 0$**

- linear potential for large quark antiquark separations, confinement.

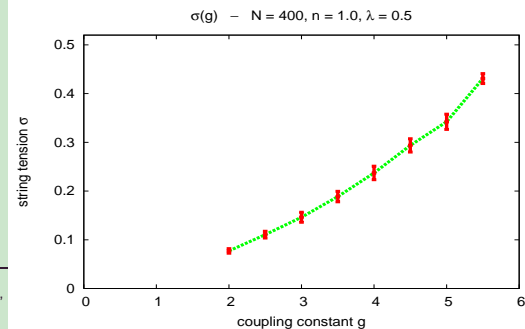
- **$\sigma$  is an increasing function of the coupling constant  $g$**

- adjust the physical scale by choosing appropriate values for  $g$ .

- **Coulomb coefficient  $\alpha > 0$**

- attractive “Coulomb-like” correction (as predicted by the bosonic string picture and by lattice calculations).

$\sigma$  plotted against  $g$



# Quark antiquark potential (4)

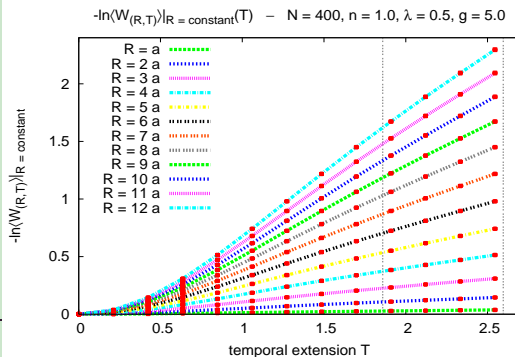
## Method 2: Calculate the quark antiquark potential directly

- For large  $T$ :

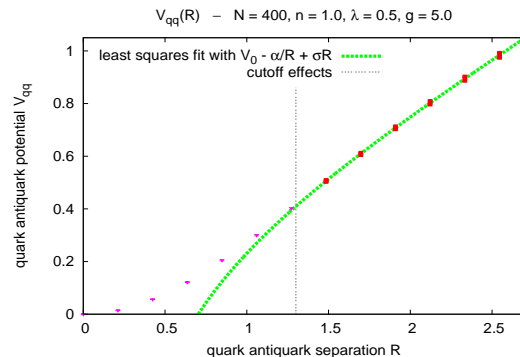
$$V_{q\bar{q}}(R)T \approx -\ln \langle W_{(R,T)} \rangle.$$

- From the slope of  $-\ln \langle W_{(R,T)} \rangle|_{R=\text{constant}}$  we can read off  $V_{q\bar{q}}(R)$ .
- Results are in agreement with our previous results.

$-\ln \langle W_{(R,T)} \rangle|_{R=\text{constant}}$  plotted against  $T$



$V_{q\bar{q}}$  plotted against  $R$



# Quantitative results

- For quantitative results, including the string tension, we need other dimensionful quantities:

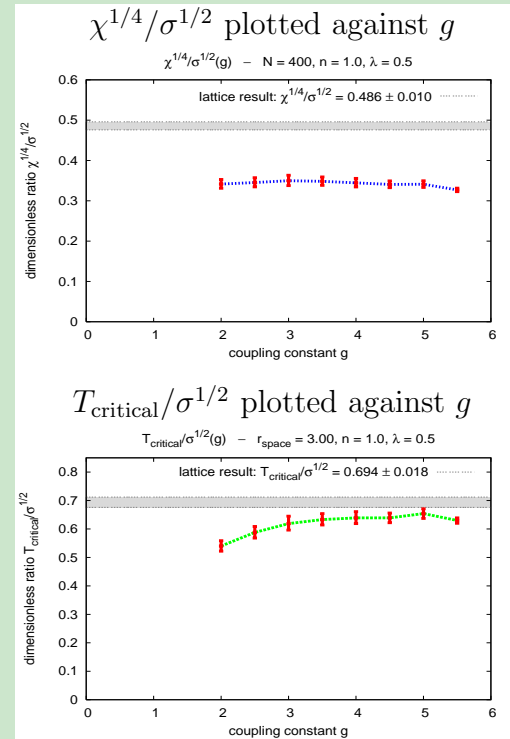
- Topological susceptibility  $\chi = \langle Q_V^2 \rangle / V$ .
- Critical temperature of the confinement deconfinement phase transition  $T_{\text{critical}}$ .

- Dimensionless quantities (physically meaningful):  
 $\chi^{1/4} / \sigma^{1/2}$  ,  $T_{\text{critical}} / \sigma^{1/2}$ .

- Consider different  $g = 2.0 \dots 5.5$  (diameter of the spacetime hypersphere 0.8 fm  $\dots$  1.9 fm).

- **Results are in qualitative agreement with results from lattice calculations.**

- **Consistent scaling behavior of  $\sigma$ ,  $\chi$  and  $T_{\text{critical}}$ .**



## Part II: properties of confining gauge field configurations

# Properties of confining gauge field ...

- **What are essential properties of confining gauge field configurations?**
- **Which gauge field configurations are responsible for confinement?**
- Apply the PP approach with different types of PPs to study the effect of different classes of gauge field configurations on confinement:
  - PPs of different size.
  - PPs with a limited range of interaction (PPs with Gaussian profile).
  - PPs without topological charge (akyrons).

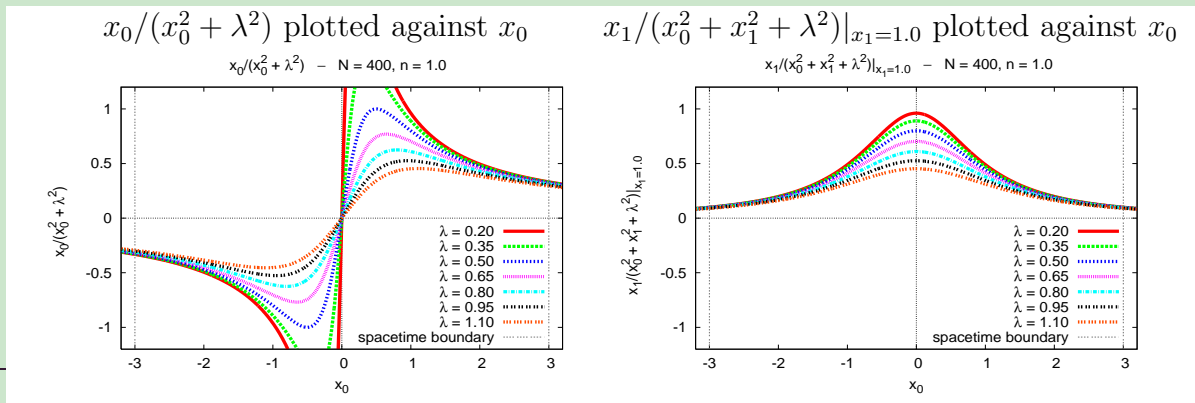
# PPs of different size (1)

- Consider ensembles with PPs of different size  $\lambda$ :

$$a_{\mu,\text{instanton}}^a(x) = \eta_{\mu\nu}^a \frac{x_\nu}{x^2 + \lambda^2}, \quad a_{\mu,\text{antiinstanton}}^a(x) = \bar{\eta}_{\mu\nu}^a \frac{x_\nu}{x^2 + \lambda^2},$$

$$a_{\mu,\text{akyon}}^a(x) = \delta^{a1} \frac{x_\mu}{x^2 + \lambda^2}.$$

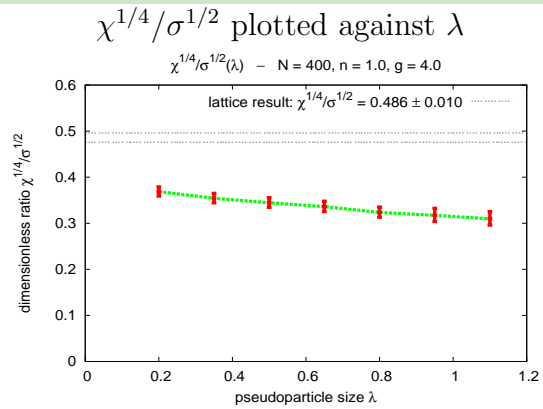
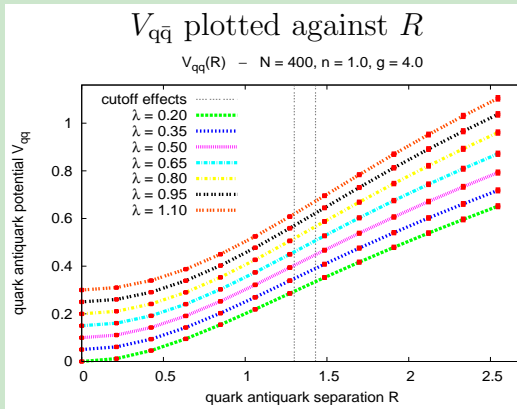
- $\lambda$  strongly affects the shape of a PP near its center but has essentially no effect on the  $1/|x|$  long range behavior.
- Typical PP profiles:





# PPs of different size (2)

- $\lambda = 0.2, \dots, 1.1$ .
- The  $q\bar{q}$  potential and the dimensionless ratio  $\chi^{1/4}/\sigma^{1/2}$  are essentially unaffected by the PP size  $\lambda$ .

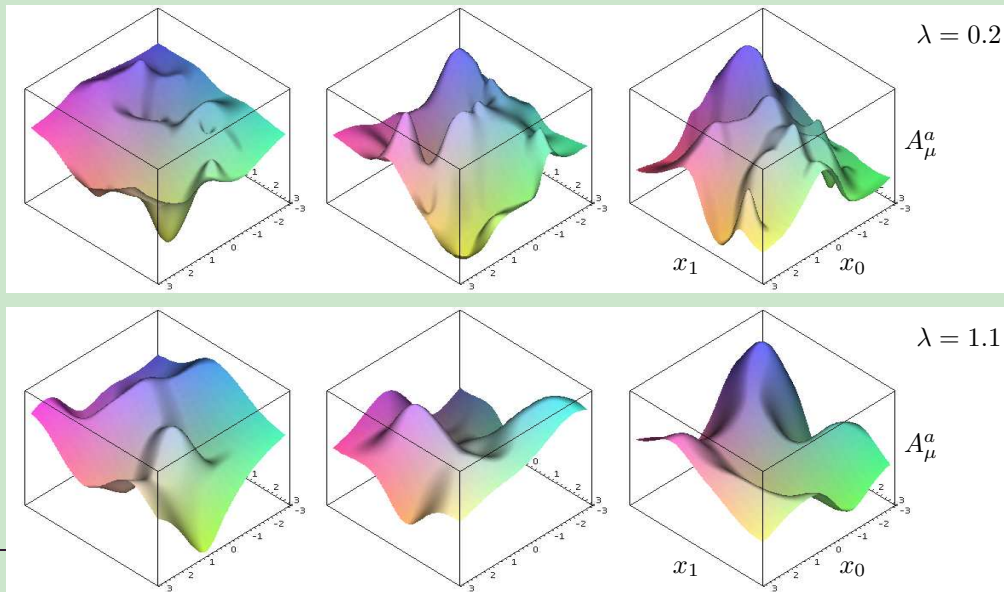


→ Confinement is a consequence of the  $1/|x|$  long range behavior of the PPs, which is unaffected by the size parameter  $\lambda$ .

# PPs of different size (3)

Typical gauge field configurations (PP size  $\lambda = 0.2 \leftrightarrow \lambda = 1.1$ )

- The global structure of typical gauge field configurations is the same.
- **For  $\lambda = 0.2$  there are additional local UV fluctuations. These UV fluctuations have no effect on confinement and the string tension.**



# PPs with Gaussian profile (1)

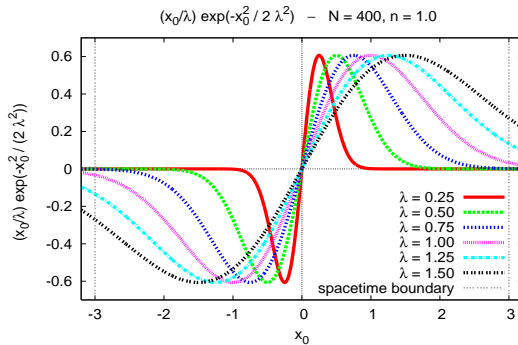
- Consider ensembles with Gaussian localized PPs of different size  $\lambda$ :

$$a_{\mu,\text{instanton}}^a(x) = \eta_{\mu\nu}^a x_\nu e^{-x^2/2\lambda^2}, \quad a_{\mu,\text{antiinstanton}}^a(x) = \bar{\eta}_{\mu\nu}^a x_\nu e^{-x^2/2\lambda^2},$$

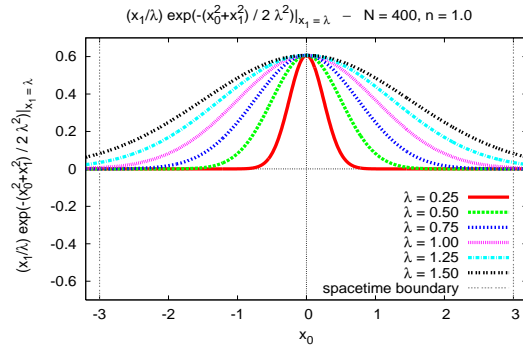
$$a_{\mu,\text{akyon}}^a(x) = \delta^{a1} x_\mu e^{-x^2/2\lambda^2}.$$

- Gaussian localized PPs have a limited range of interaction, which is proportional to their size  $\lambda$ .**
- Typical PP profiles:

$(x_0/\lambda)\exp(-x_0^2/2\lambda^2)$  plotted against  $x_0$

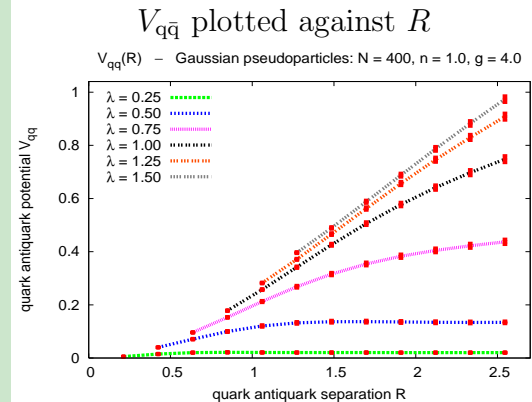
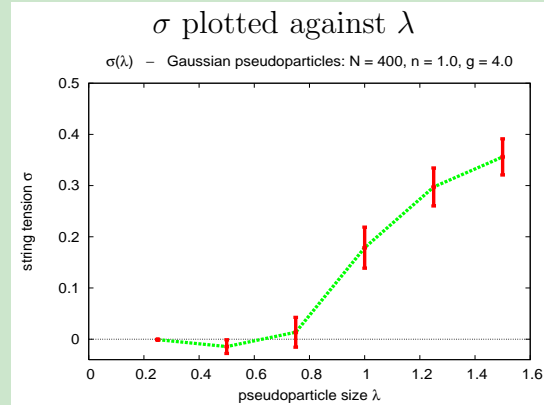
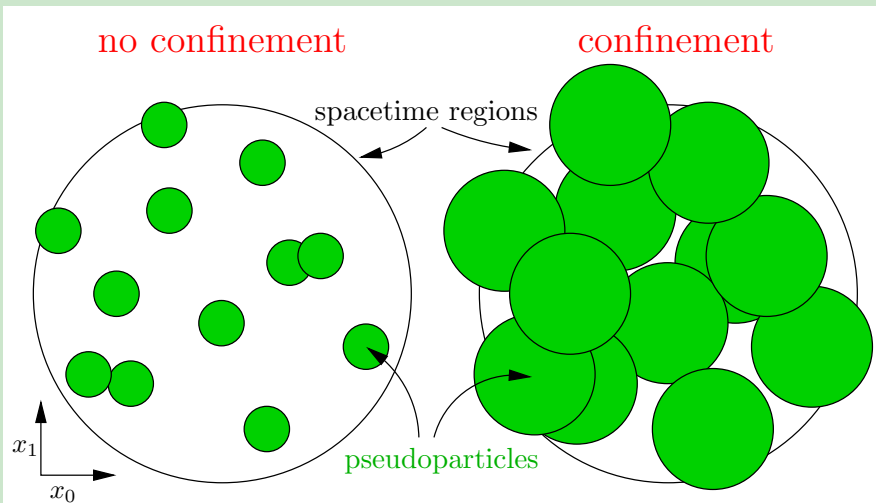


$(x_1/\lambda)\exp(-(x_0^2 + x_1^2)/2\lambda^2)|_{x_1=\lambda}$  plotted against  $x_0$



# PPs with Gaussian profile (2)

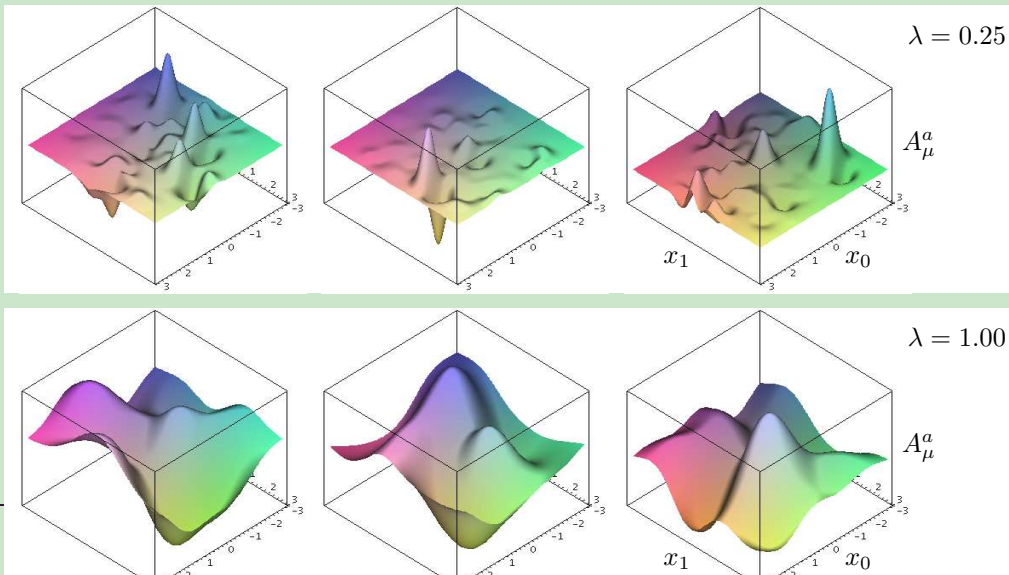
- Short range PPs ( $\lambda \leq 0.50$ )
  - little overlap between neighboring PPs.
  - no confinement.
- Long range PPs ( $\lambda \geq 1.00$ )
  - significant overlap between neighboring PPs.
  - confinement.
- **PP percolation**  $\leftrightarrow$  **confinement.**



# PPs with Gaussian profile (3)

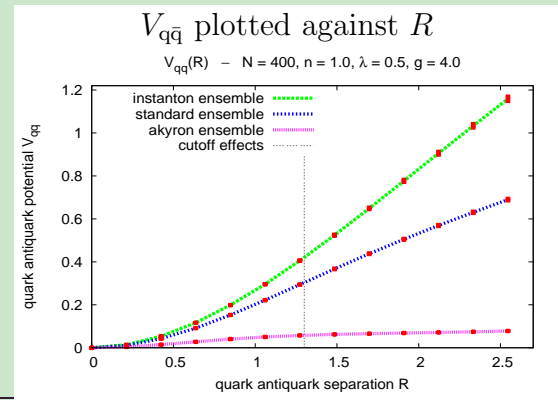
Typical gauge field configurations ( $\lambda = 0.25 \leftrightarrow \lambda = 1.00$ )

- $\lambda = 0.25$ : local UV fluctuations  $\rightarrow$  no confinement.
- $\lambda = 1.00$ : global excitations  $\rightarrow$  confinement.
- **Gauge field configurations responsible for confinement contain extended structures and large area excitations.**



# Instantons, antiinstantons and akyrons

- Consider the following ensembles:
  - Akyron ensemble: 400 akyrons (**topological charge density  $q = 0$** ).
  - Standard ensemble: 150 instantons, 150 antiinstantons, 100 akyrons.
  - Instanton ensemble: 200 instantons, 200 antiinstantons.
- No confinement in the akyron ensemble
  - akyrons alone are not suited to reproduce Yang-Mills physics.
  - **supports the expectation that confinement and topological charge are closely related.**
- Standard ensemble  $\leftrightarrow$  instanton ensemble
  - $(\chi^{1/4}/\sigma^{1/2})_{\text{standard}} = 0.35$
  - $(\chi^{1/4}/\sigma^{1/2})_{\text{instanton}} = 0.26$
  - $(\chi^{1/4}/\sigma^{1/2})_{\text{lattice}} = 0.49.$
  - **using akyrons is beneficial with respect to quantitative results.**



# Part III: fermionic fields in the pseudoparticle approach (first steps)

# Basic principle (fermionic fields) (1)

- **How can fermions be included in the PP approach?**
- Action and partition function of **any theory with quadratic fermion interaction** (no restriction to SU(2) Yang-Mills theory anymore):

$$S[\psi, \bar{\psi}, \phi] = \int dx \left( \bar{\psi} Q(\phi) \psi + \mathcal{L}(\phi) \right)$$

$$Z = \int D\psi D\bar{\psi} D\phi e^{-S[\psi, \bar{\psi}, \phi]}$$

( $Q$ : Dirac operator;  $\phi$ : any type and number of bosonic fields, e.g. the non-Abelian gauge field in QCD).



# Basic principle (fermionic fields) (2)

- Consider only those fermionic field configurations, which can be represented by a linear superposition a fixed number of localized building blocks:

$$\psi(x) = \sum_j \underbrace{\eta_j G_j(x)}_{j\text{-th PP}}$$

( $\eta_j$ : Grassmann valued spinors;  $G_j$ : functions, which are localized in space as well as in time, i.e. PPs).

- Define the functional integration over all fermionic field configurations as an integration over the Grassmann valued spinors:

$$\int D\psi D\bar{\psi} \dots = \int \left( \prod_j d\eta_j d\bar{\eta}_j \right) \dots$$

# Basic principle (fermionic fields) (3)

- Integrate out the fermions:

$$S_{\text{effective}}[\phi] = \int d^{d+1}x \mathcal{L}(\phi) - \ln \left( \det \left( \langle G_j | Q | G_{j'} \rangle \right) \right)$$

$$Z \propto \int D\phi e^{-S_{\text{effective}}[\phi]}$$

( $\langle G_j | Q | G_{j'} \rangle$  is a finite matrix; **“Q-regularization”**).

- If  $\det(Q)$  is real and positive,  $\det(Q) = \sqrt{\det(Q^\dagger Q)}$ . This suggests another PP regularization:

$$S_{\text{effective}}[\phi] = \int d^{d+1}x \mathcal{L}(\phi) - \frac{1}{2} \ln \left( \det \left( \langle G_j | Q^\dagger Q | G_{j'} \rangle \right) \right)$$

(**“ $Q^\dagger Q$ -regularization”**).

- **The “ $Q^\dagger Q$ -regularization” has significant advantages over the naive “Q-regularization”.**

# $Q$ versus $Q^\dagger Q$ (1)

- For the sake of simplicity: consider all PPs  $G_j$  to be orthonormal, i.e.  $\langle G_j | G_{j'} \rangle = \delta_{jj'}$  (this is not a restriction!).
- The problem of the  $Q$ -regularization:
  - **Applying the Dirac operator  $Q$  to one of the PPs  $G_{j'}$  in general yields a function, which is (partially) outside the PP function space  $\text{span}\{G_n\}$ , i.e.**

$$QG_{j'}(x) = \sum_k a_{j'k} G_k(x) + h_{j'} H_{j'}(x)$$

**( $H_{j'}$  normalized,  $H_{j'} \perp \text{span}\{G_n\}$ ).**

- If  $|\sum_k a_{j'k} G_k| \gg |h_{j'}| \rightarrow$  no problem.
- If  $|\sum_k a_{j'k} G_k| \lesssim |h_{j'}| \rightarrow$  when computing the fermionic matrix  $\langle G_j | Q | G_{j'} \rangle$ , a significant part of  $QG_{j'}$  is simply ignored, just because  $H_{j'}$  is perpendicular to the PP function space  $\text{span}\{G_n\}$ .

## $Q$ versus $Q^\dagger Q$ (2)

- The advantage of the  $Q^\dagger Q$ -regularization:
  - **Both the left hand sides  $\langle G_j | Q^\dagger$  and the right hand sides  $Q | G_{j'} \rangle$  of the matrix elements  $\langle G_j | Q^\dagger Q | G_{j'} \rangle$  might be outside the PP function space  $\text{span}\{G_n\}$ , but they form the same function space,  $\text{span}\{QG_n\}$ , in which their overlap is computed.**
- For “better arguments” cf. M. Wagner, arXiv:0704.3023 [hep-lat].

# Testing ground: Gross-Neveu model (1)

- Action and partition function of the 1+1-dimensional Gross-Neveu model:

$$S = \int d^2x \left( \sum_{n=1}^N \bar{\psi}^{(n)} \left( \gamma_0 (\partial_0 + \mu) + \gamma_1 \partial_1 \right) \psi^{(n)} - \frac{g^2}{2} \left( \sum_{n=1}^N \bar{\psi}^{(n)} \psi^{(n)} \right)^2 \right)$$

$$Z = \int \left( \prod_{n=1}^N D\psi^{(n)} D\bar{\psi}^{(n)} \right) e^{-S}$$

( $N$ : number of flavors;  $\mu$ : chemical potential;  $g$ : coupling constant).

# Testing ground: Gross-Neveu model (2)

- Introduce a real scalar field  $\sigma$  and integrate out the fermions:

$$S_{\text{effective}} = N \left( \frac{1}{2\lambda} \int d^2x \sigma^2 - \ln \left( \det \left( \gamma_0(\partial_0 + \mu) + \gamma_1 \partial_1 + \sigma \right) \right) \right)$$

$$Z \propto \int D\sigma e^{-S_{\text{effective}}}$$

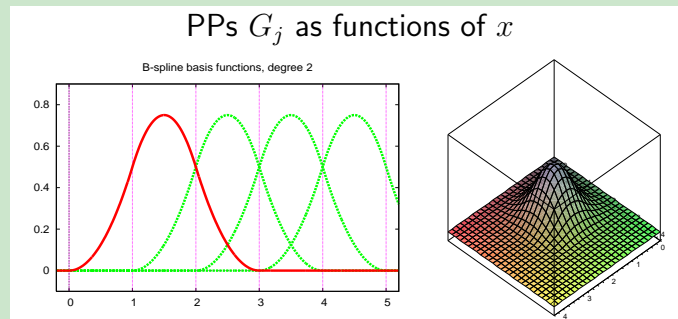
$$(\lambda = Ng^2).$$

- Large- $N$  limit:

- $N \rightarrow \infty$ ,  $\lambda = Ng^2 = \text{constant}$ .
- There is no need to compute the  $\sigma$ -path integral anymore.
- It is sufficient to minimize  $S_{\text{effective}}$  with respect to  $\sigma$ .
- $\sigma = -g^2 \sum_{n=1}^N \bar{\psi}^{(n)} \psi^{(n)}$  (chiral condensate).

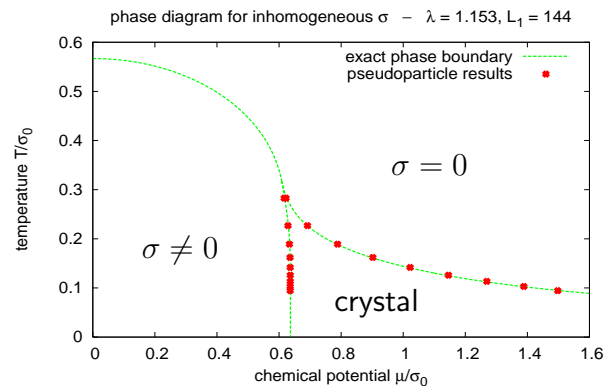
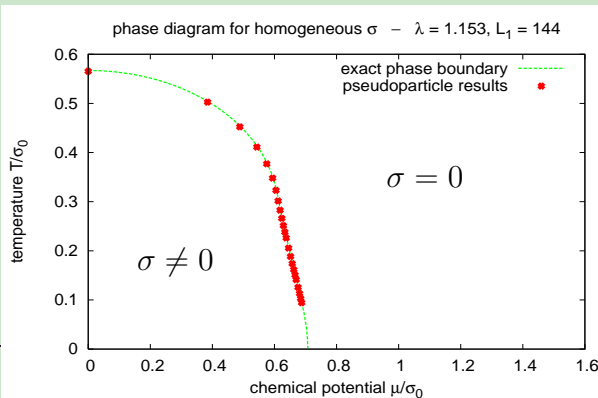
# Fermionic PPs

- Fermionic PPs in this talk: a large number of uniformly distributed “hat functions” (B-spline basis functions of degree 2).
  - “Sensible set of field configurations” (any not too heavily oscillating field configuration can be approximated)
    - we can expect to reproduce correct Gross-Neveu results.
  - Piecewise polynomial functions
    - certain integrals can be calculated analytically.



# Phase diagram

- **$Q$ -regularization: completely wrong and useless results.**
  - No improvement, when using a larger number of PPs.
  - No improvement, when using a different type of PPs.
- **$Q^\dagger Q$ -regularization: excellent agreement with analytical results.**
  - Homogeneous chiral condensate: analytical results by U. Wolff, 1985.
  - Inhomogeneous chiral condensate: analytical results by O. Schnetz, M. Thies, K. Urlichs, 2004.

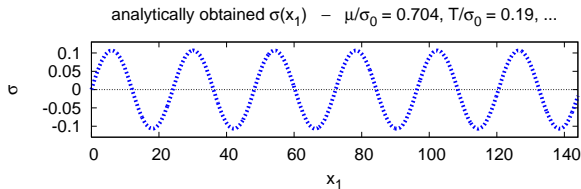
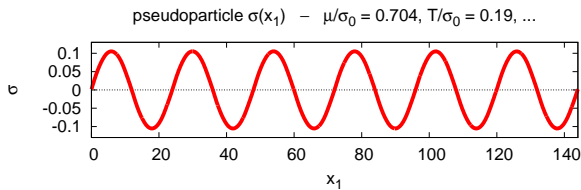




# Chiral condensate

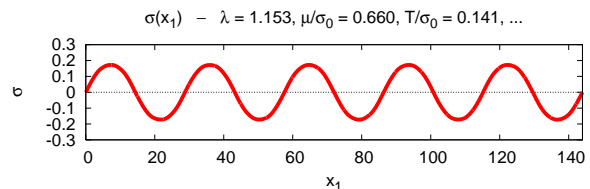
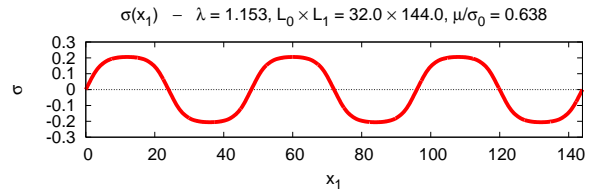
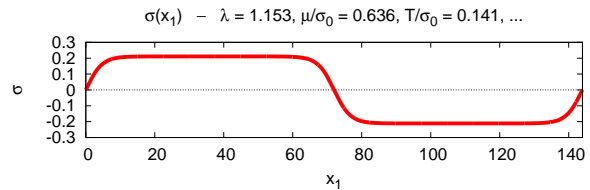
- $Q^\dagger Q$ -regularization: excellent agreement with analytical results.
  - The sin-like behavior “inside the crystal phase” changes to a kink-antikink structure, when approaching the left phase boundary.

PP result



analytical result

close to the left phase boundary



inside the crystal phase

# Summary and Outlook

# Summary and conclusions (1)

- The PP approach with  $\approx 400$  instantons, antiinstantons and akyrons is able to reproduce many essential features of SU(2) Yang-Mills theory:
  - **Linear quark antiquark potential, i.e. confinement.**
  - **Consistent scaling behavior of  $\sigma$ ,  $\chi$  and  $T_{\text{critical}}$ .**
  - Dimensionless quantities  $\chi^{1/4}/\sigma^{1/2}$ ,  $T_{\text{critical}}/\sigma^{1/2}$  are in qualitative agreement with results from lattice calculations.
- Essential properties of confining gauge field configurations:
  - Long range PPs necessary for confinement (PP percolation)
    - **confinement  $\leftrightarrow$  extended structures and large area excitations.**
  - Instantons and antiinstantons (PPs with non-vanishing topological charge density) necessary for confinement
    - **confinement  $\leftrightarrow$  topological charge.**
  - Short range behavior of PPs irrelevant for confinement
    - **confinement not affected by UV fluctuations.**

# Summary and conclusions (2)

- Inclusion of fermions in the PP approach:
  - Always apply the  $Q^\dagger Q$ -regularization and not the naive  $Q$ -regularization.
  - The application of the PP approach to compute the phase diagram of the 1+1-dimensional Gross-Neveu model in the large- $N$ -limit has been a successful test.
  - Next steps:
    - \* Apply the PP approach to QCD.
    - \* Try to identify a small number of physically relevant fermionic PPs (PPs, which are able to approximate the low lying eigenmodes of the Dirac operator?).

# Outlook

- Current research:
  - Improve the static quark antiquark potential:
    - \* Use improved operators (smeared Wilson loops) to extract the static quark antiquark potential (o.k.).
    - \* Casimir scaling for higher quark representations (o.k.).
    - \* String breaking for the adjoint representation (???)
  - Consider  $SU(2)$  Yang-Mills theory with dynamical fermions:
    - \* Chiral symmetry breaking by computing the low lying eigenmodes of the Dirac operator in the quenched approximation (Banks-Casher relation) (???)
- Goal: obtain a model with a small number of degrees of freedom, which exhibits chiral symmetry breaking and a confinement deconfinement phase transition at the same time.
- Compute further observables: pion masses, ...